Polymer Testing 135 (2024) 108445

Contents lists available at ScienceDirect

Polymer Testing

journal homepage: www.elsevier.com/locate/polytest

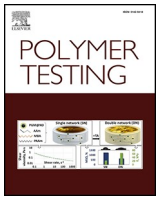

Enhanced thermal properties of tensile-aligned chopped carbon Fiber/HDPE composites for one-directional thermal ventilation

Gu-Hyeok Kang [a], Myungsoo Kim [c,**], Young-Bin Park [a,b,*]

[a] Department of Mechanical Engineering, Ulsan National Institute of Science and Technology (UNIST), UNIST-gil 50, Ulju-gun, Ulsan, 44919, Republic of Korea
[b] Fraunhofer Project Center for Composites Research @ UNIST, UNIST-gil 50, Ulju-gun, Ulsan, 44919, Republic of Korea
[c] Department of Mechanical and Automotive Engineering, Youngsan University, 288 Junam-ro, Yangsan-si, Kyungsangnam-do, 50510, Republic of Korea

ARTICLE INFO

Keywords:
Chopped carbon fiber
High-density polyethylene composite
Fiber alignment
Draw ratio
Thermal conductivity
Simulation

ABSTRACT

This study was aimed at enhancing the thermal properties of unidirectional chopped carbon fiber (CCF)/high-density polyethylene (HDPE) composites for applications requiring unidirectional heat dissipation. CCF/HDPE composite samples were fabricated using a special post-extrusion tension alignment method. The influence of different manufacturing variables, including fiber content, length, and draw ratio (DR, representing the tension), on the thermal conductivity was examined. Moreover, the response surface methodology (RSM) was used to investigate the influence of the manufacturing process variables. Results indicated that the thermal conductivity increased with increasing CCF wt.% and DR. The increase in DR promoted fiber alignment, contributing to enhanced thermal conductivity in the aligned direction. Additionally, the thermal conductivity increased with the increase in the CCF length. The proposed approach can facilitate efficient heat management in automotive and aerospace industries.

1. Introduction

Effective heat management has recently emerged as a crucial requirement in various industrial sectors, including automotive, aerospace, electronics, and renewable energy [1–3]. Excessive heat accumulation can compromise the performance, reliability, and lifespan of critical components, leading to decreased efficiency and increased maintenance costs [4,5]. Consequently, the development of composite materials with enhanced thermal characteristics has garnered significant interest from both researchers and industry experts [6–8].

In this context, various researchers have focused on the thermal conductivity of composites based on their internal structures. For example, Zhou et al. analyzed the influence of a multi-level assembly design incorporating carbon fiber, polyaniline nanofiber, and one-dimensional silver nanowire materials on the formation of a "branch–trunk' interlocked internal structure. Such structures, spanning macro to micro sizes, have been applied in both electromagnetic shielding and thermal management [9]. Ibrahim et al. used both experimental and analytical modeling techniques to examine the thermal conductivity based on the arrangement of chopped carbon fibers used in three-dimensional (3D) printing, clarifying the influence of fiber direction and volume fraction on the effective thermal conductivity [10]. Despite their effectiveness, methods for inducing structures through multi-level assembly are excessively complex, and 3D printing is impractical for producing large structures.

A promising approach for managing the thermal properties of composites is to integrate chopped carbon fibers (CCF) into a high-density polyethylene (HDPE) matrix. The thermal and mechanical properties of such structures considerably depend on the quantity and length of fibers, as well as their dispersion, and must thus be optimized [11–13]. Owing to the anisotropic nature of CCF, the fiber orientation significantly influences its properties. In particular, aligning these chopped carbon fibers under tension within the composite structure can further enhance its thermal characteristics. According to theoretical research, the mechanical properties associated with fiber orientations of 0° and 90° are over three times different. Thus, the matrix strength can be enhanced through coupling with over-molded plastic components.

Moreover, the recent emphasis on mass production to enhance cost competitiveness and production speed requires relevant research to focus on not only composite materials but also production aspects,

* Corresponding author. Department of Mechanical Engineering, Ulsan National Institute of Science and Technology (UNIST), UNIST-gil 50, Ulju-gun, Ulsan, 44919, Republic of Korea.
** Corresponding author.
E-mail addresses: mskim@ysu.ac.kr (M. Kim), ypark@unist.ac.kr (Y.-B. Park).

https://doi.org/10.1016/j.polymertesting.2024.108445
Received 1 March 2024; Received in revised form 15 April 2024; Accepted 2 May 2024
Available online 3 May 2024

Table 1
HDPE extruder process temperatures.

	Zone 1	Zone 2	Zone 3	Zone 4	Zone 5	Zone 6
Temperature (°C)	70	90	150	210	210	170

encompassing suitable manufacturing methods, material selection, and thermal energy management.

Considering these aspects, this study was aimed at enhancing the thermal properties of unidirectionally aligned CCF/HDPE composites for applications requiring unidirectional heat dissipation. Through a special post-extrusion tension alignment method, the fibers in the composite samples were aligned, and the thermal conductivity was measured and analyzed for various fiber contents, lengths, and draw ratios (DR) representing the tension. Moreover, using the response surface methodology (RSM), regression models for thermal conductivity were constructed to analyze the degrees of influence of the manufacturing parameters and provide an industrially applicable foundation for predicting and enhancing the thermal conductivity.

2. Experimental procedure

2.1. Materials

Discontinuous fiber-reinforced composites, incorporating CCF (SYC-TR-PU, Sunyoung Industry, Yangsan, South Korea) and HDPE (HDPE B230A, Hanwha Total, Seosan, South Korea), were used. Fibers with a diameter of 7 μm and lengths of 1, 3, 6, and 12 mm, were pelletized with a polyurethane binder. The polymer exhibited a molecular weight of 300,000 and density of 0.963 g/cm3.

2.2. Processing

From bound CCF, split CCF was obtained through ultrasonication with methanol. Subsequently, both the CCF and HDPE underwent vacuum drying at 80 °C for 12 h to eliminate residual moisture. The dried fibers and polymer pellets were blended and extruded using a single-screw extruder (Ocean OC-200, China). The extrusion process involved charging, mixing, and extrusion stages, conducted for 5 min at 40 rpm, 10 min at 150 rpm, and 60 min at 150 rpm, respectively. The processing temperature was meticulously controlled across Zones 1–6, as specified in Table 1. As shown in Fig. 1, the extruded filament was modified by adjusting the extrusion and rotation speeds of the first and second take-up rolls. The thickness of each extruded filament was measured and adjusted to achieve the desired DR. This comprehensive manufacturing process laid the foundation for the subsequent investigation of the thermal properties of CCF/HDPE composites.

2.3. Sampling

To measure the thermal conductivity of CCF/HDPE composite filaments aligned in a specific direction, specimens were unidirectionally stacked, as shown in Fig. 2, and subjected to heat compression at 150 °C under 5 MPa using a mold (10 mm × 10 mm × 150 mm). Subsequently, the specimens were subjected to water-jet cutting to fit the holder size (10 mm × 10 mm × 2 mm) of the LFA447 (LFA 447 NanoFlash®, Netzsch, Germany) tool. Tensile specimens were prepared under various conditions, including four fiber concentrations (2.5, 5.0, 7.5, 10.0 wt%), four fiber lengths (1, 3, 6, 12 mm), and three DRs (1.0, 1.5, 2.0).

2.4. Characterization

To assess the thermal conductivity of the aligned CCF/HDPE composites, the LFA447 tool was used for measuring the thermal diffusivity and specific heat, and a porosimetry system was used for measuring the density. The thermal conductivity was calculated as

$$k = \frac{\alpha}{\rho \bullet C_p} \quad (1)$$

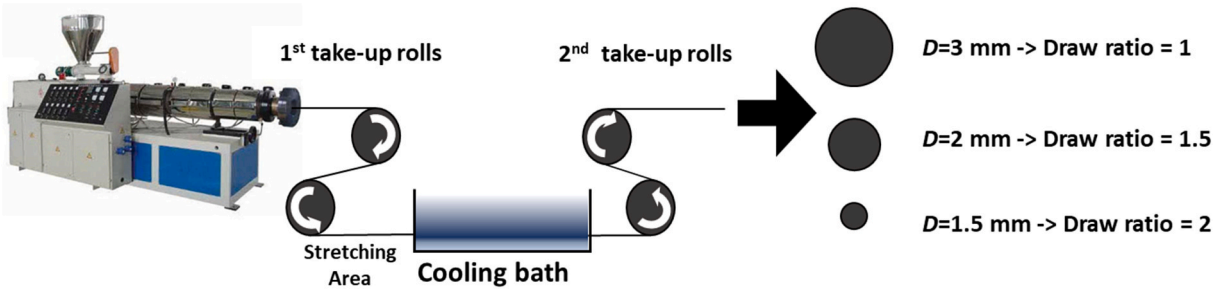

Fig. 1. Schematic of influence of filament dimension on draw ratio.

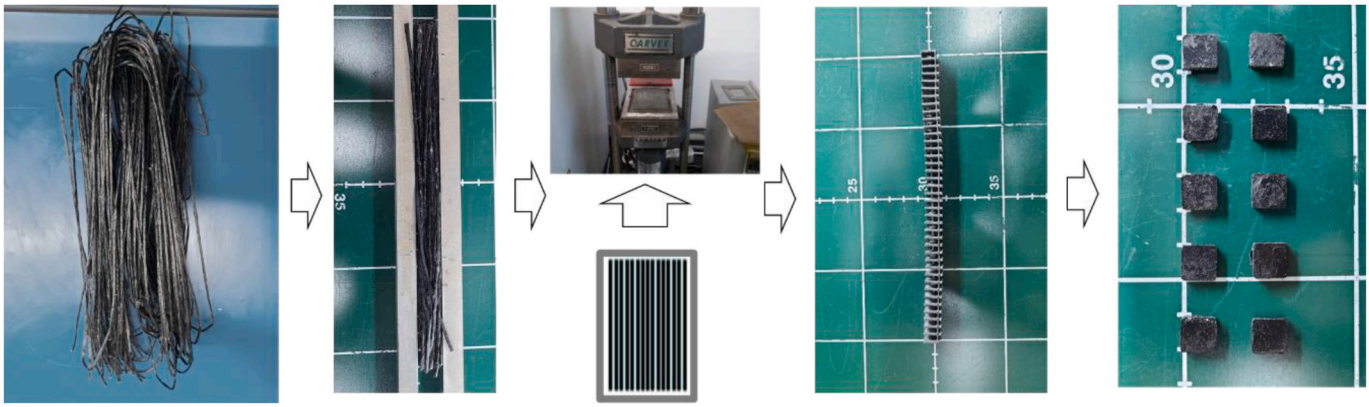

Fig. 2. Manufacturing of aligned chopped carbon fiber (CCF)/HDPE composite specimen for thermal conductivity measurements.

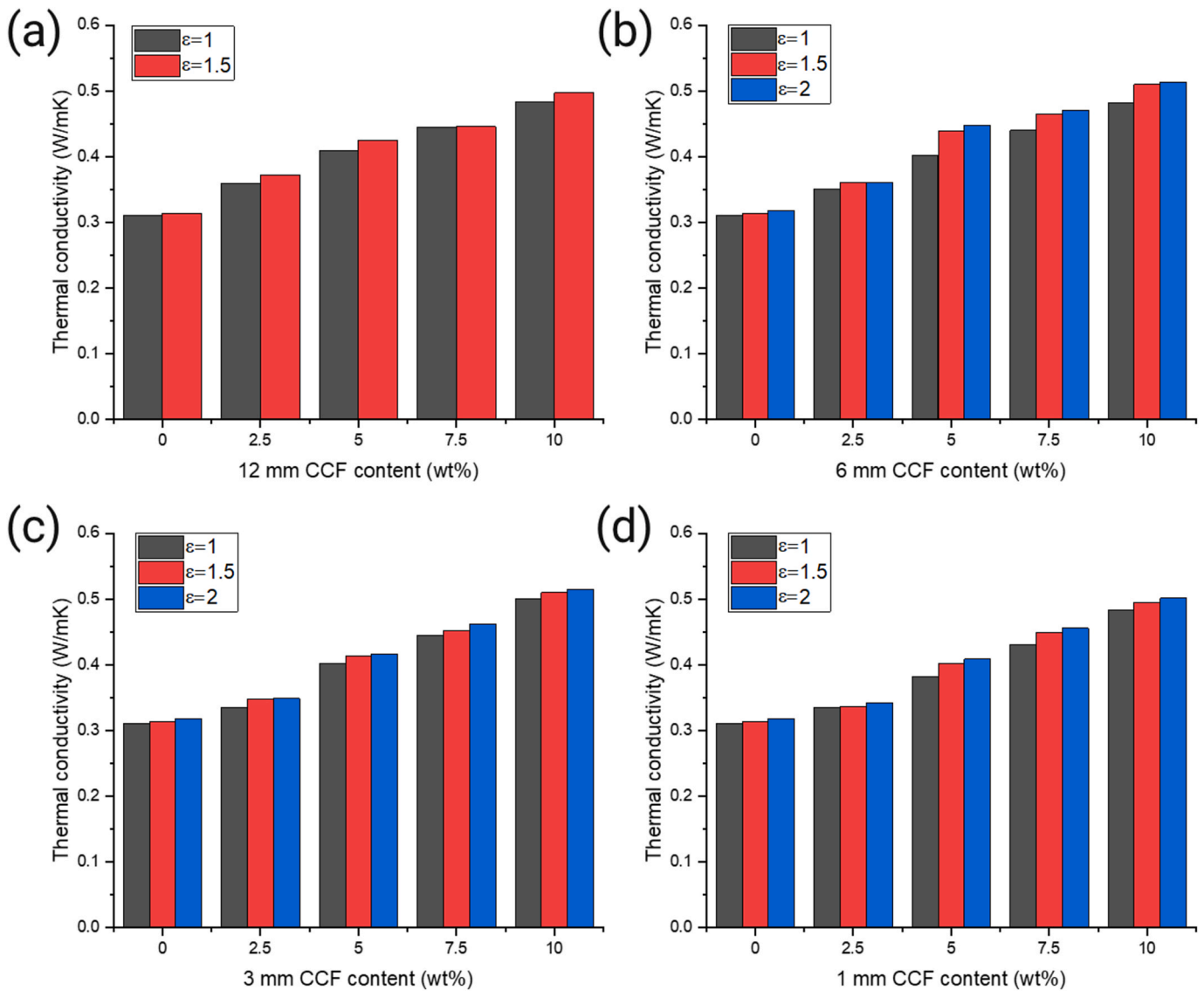

Fig. 3. Thermal conductivity with draw ratio (DR) at (a) 12 mm, (b) 6 mm, (c) 3 mm, and (d) 1 mm of CCF length.

Table 2
Thermal conductivity results (unit: W/m·K).

Composite Samples	CCF wt.%	DR		
		1	1.5	2
Pure HDPE	0	0.31004	0.31396	0.31802
1 mm	2.5	0.33475	0.3359	0.34204
	5	0.38128	0.40128	0.40852
	7.5	0.43043	0.44859	0.45543
	10	0.48354	0.49518	0.5013
3 mm	2.5	0.3353	0.34753	0.34854
	5	0.40152	0.41368	0.41677
	7.5	0.44527	0.45156	0.46156
	10	0.49966	0.50966	0.51467
6 mm	2.5	0.35042	0.36042	0.36042
	5	0.40213	0.43852	0.44767
	7.5	0.4398	0.46527	0.47043
	10	0.4813	0.50966	0.513
12 mm	2.5	0.35897	0.37186	–
	5	0.40852	0.4249	–
	7.5	0.44527	0.44559	–
	10	0.48354	0.49742	–

where α is the thermal diffusivity, representing the rate of heat transfer through a material; ρ is the density; and C_p represents the heat capacity of the substance. The laser flash method, based on rapid and controlled heating of a material using a short-duration laser pulse, was used to determine the thermal diffusivity from the measured temperature response of the sample. Additionally, scanning electron microscopy (SEM) was used to investigate the aligned morphology of CCF in the composites.

2.5. RSM

The thermal conductivity was analyzed using the RSM, which explores the change in thermal conductivity according to variations in the design variables. This approach facilitated a comparison with the measurement results.

Notably, for RSM analysis and prediction of thermal conductivity, an empirical regression model based on experimental data must be established [11]. In this study, a linear regression model with two independent manufacturing variables was used:

$$y = \beta_0 + \beta_1 x_1 + \beta_2 x_2 + \varepsilon \quad (2)$$

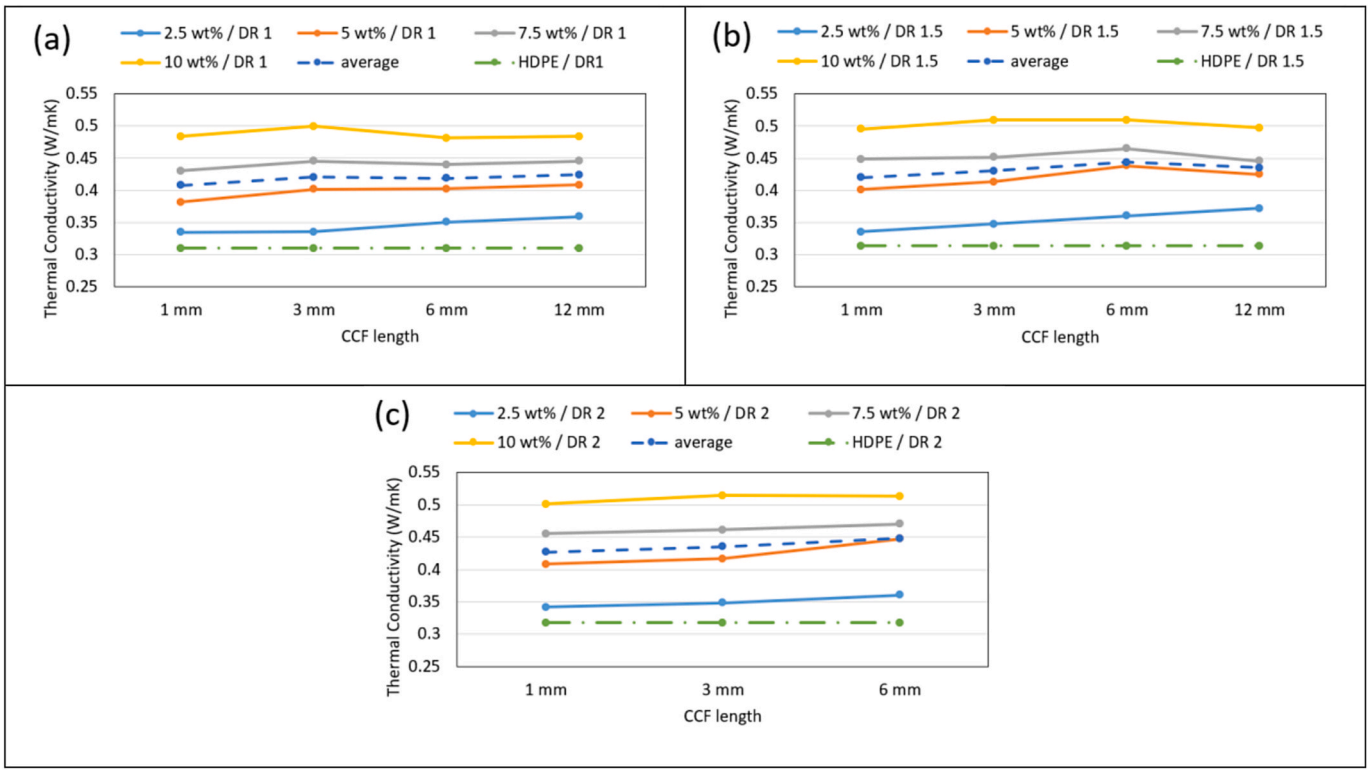

Fig. 4. Change in thermal conductivity with CCF length and content at DR = (a) 1, (b) 1.5, (c) 2, The average was obtained from the results of the composites without pure-HDPE sample.

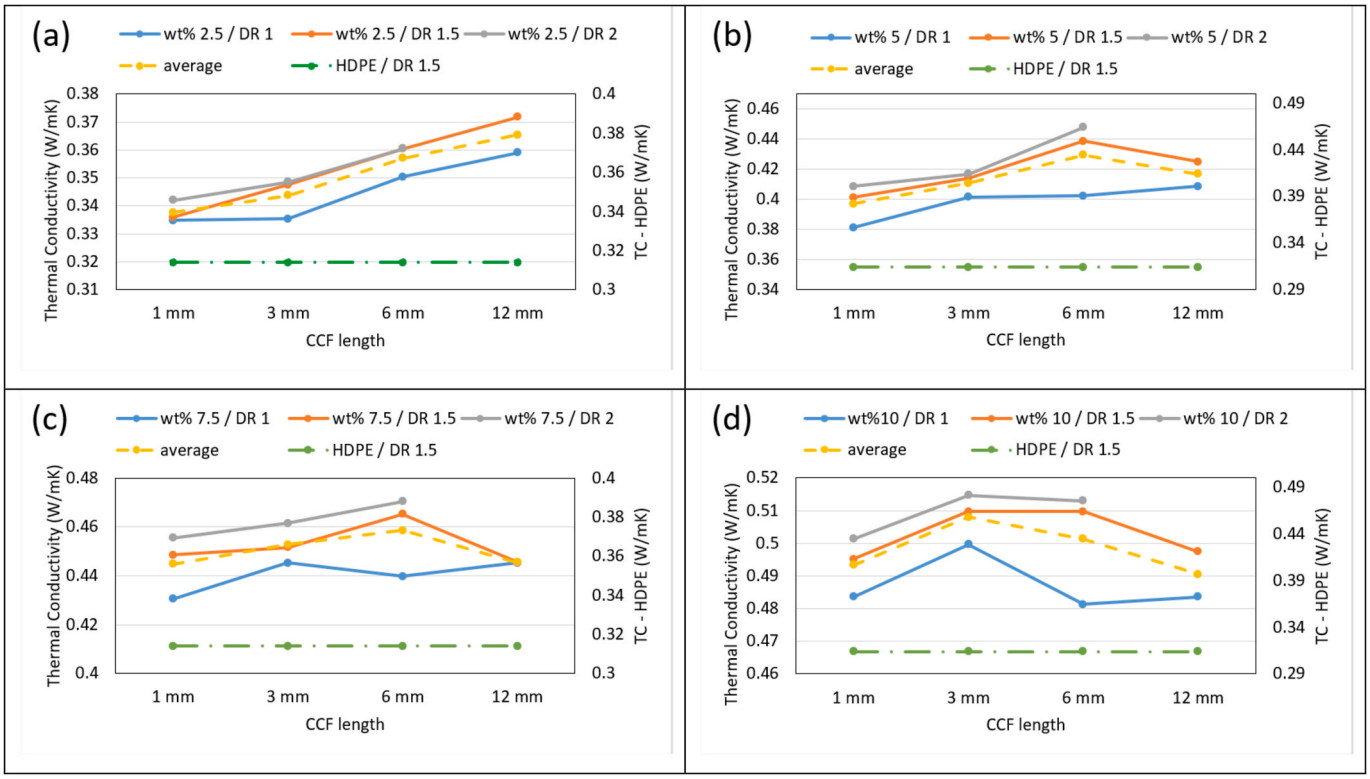

Fig. 5. Change in thermal conductivity with CCF length and DR at CCF content (wt.%) = (a) 2.5, (b) 5, (c) 7.5, (d) (a) 10, The average was obtained from the results of the composites without pure-HDPE sample.

Table 3
Least squares estimators (vector **b**) for each sample.

1 mm	3 mm	6 mm	12 mm
$\begin{bmatrix}0.2786\\0.0186\\0.0171\end{bmatrix}$	$\begin{bmatrix}0.2861\\0.0199\\0.0136\end{bmatrix}$	$\begin{bmatrix}0.2791\\0.0190\\0.0252\end{bmatrix}$	$\begin{bmatrix}0.2949\\0.0175\\0.0190\end{bmatrix}$

where y is the response (thermal conductivity in this work); and x_1 and x_2 represent the CCF wt.% and DR, respectively. β_0, β_1, β_2 are regression coefficients, and ε is a term that represents other sources of variability, such as measurement errors.

For n observations, Eq. (2) can be rewritten as

$$y_i = \beta_0 + \beta_1 x_{i1} + \beta_2 x_{i2} + \varepsilon_i, i = 1, 2, \ldots, n \tag{3}$$

Equation (3) may be written in matrix notation as follows:

$$\mathbf{y} = \mathbf{X\beta} + \boldsymbol{\varepsilon} \tag{4}$$

The objective is to obtain the vector of least-squares estimators, **b**, which minimizes

$$\begin{aligned} L &= \sum_{i=1}^{n} \varepsilon_i^2 = \boldsymbol{\varepsilon}^{\mathrm{T}}\boldsymbol{\varepsilon} = (\mathbf{y} - \mathbf{X\beta})^{\mathrm{T}}(\mathbf{y} - \mathbf{X\beta}) \\ &= \mathbf{y}'\mathbf{y} - 2\beta'\mathbf{X}'\mathbf{y} + \beta'\mathbf{X}'\mathbf{X\beta} \end{aligned} \tag{5}$$

Therefore, the least-squares estimators must satisfy the following criterion:

$$\left.\frac{\partial L}{\partial \beta}\right|_{\mathbf{b}} = -\mathbf{X}^{\mathrm{T}}\mathbf{y} + \mathbf{X}^{\mathrm{T}}\mathrm{Xb} = 0 \tag{6}$$

Thus, the least squares estimator of β can be expressed as

$$\mathbf{b} = \left(\mathbf{X}^{\mathrm{T}}\mathbf{X}\right)^{-1}\mathbf{X}^{\mathrm{T}}\mathbf{y} \tag{7}$$

The fitted regression model is then

$$\hat{\mathbf{y}} = \mathbf{Xb} \tag{8}$$

This model was used to analyze thermal conductivities with respect to CCF wt% and DR. The discrepancy between the observed value y_i and estimated value $\hat{y}_i$, i.e., the residual e_i is defined as $e_i = y_i - \hat{y}_i$. The n × 1 vector of residuals can be expressed as

$$\mathbf{e} = \mathbf{y} - \hat{\mathbf{y}} \tag{9}$$

Detailed derivations for the abovementioned expressions can be found elsewhere [14].

3. Results and discussion

3.1. Thermal conductivity analysis

Fig. 3 and Table 2 summarize the results of thermal conductivity.

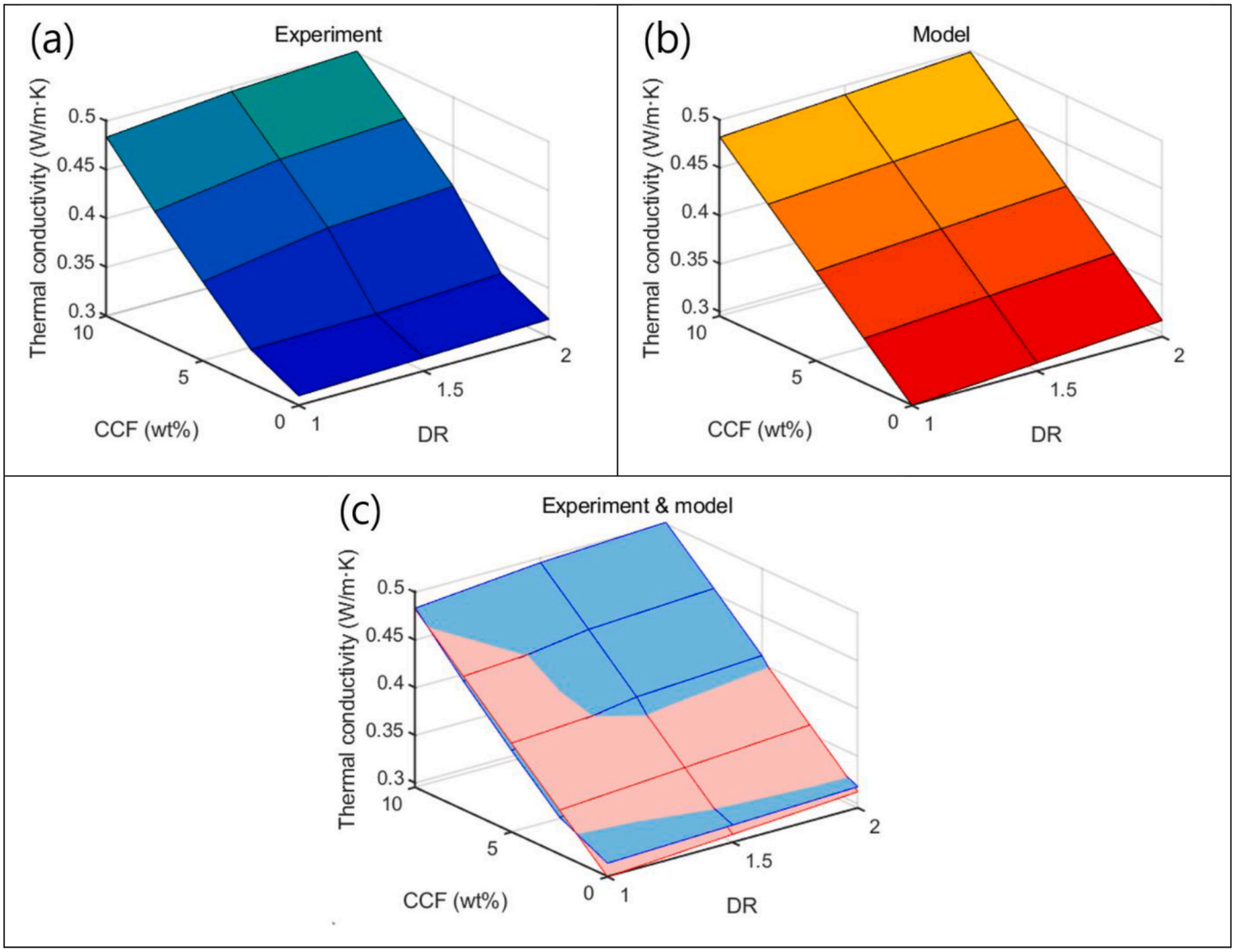

Fig. 6. Thermal conductivity of composites with 1 mm-CCF, obtained through (a) experiment, (b) model presented in Eq. (9), (c) experiment and model.

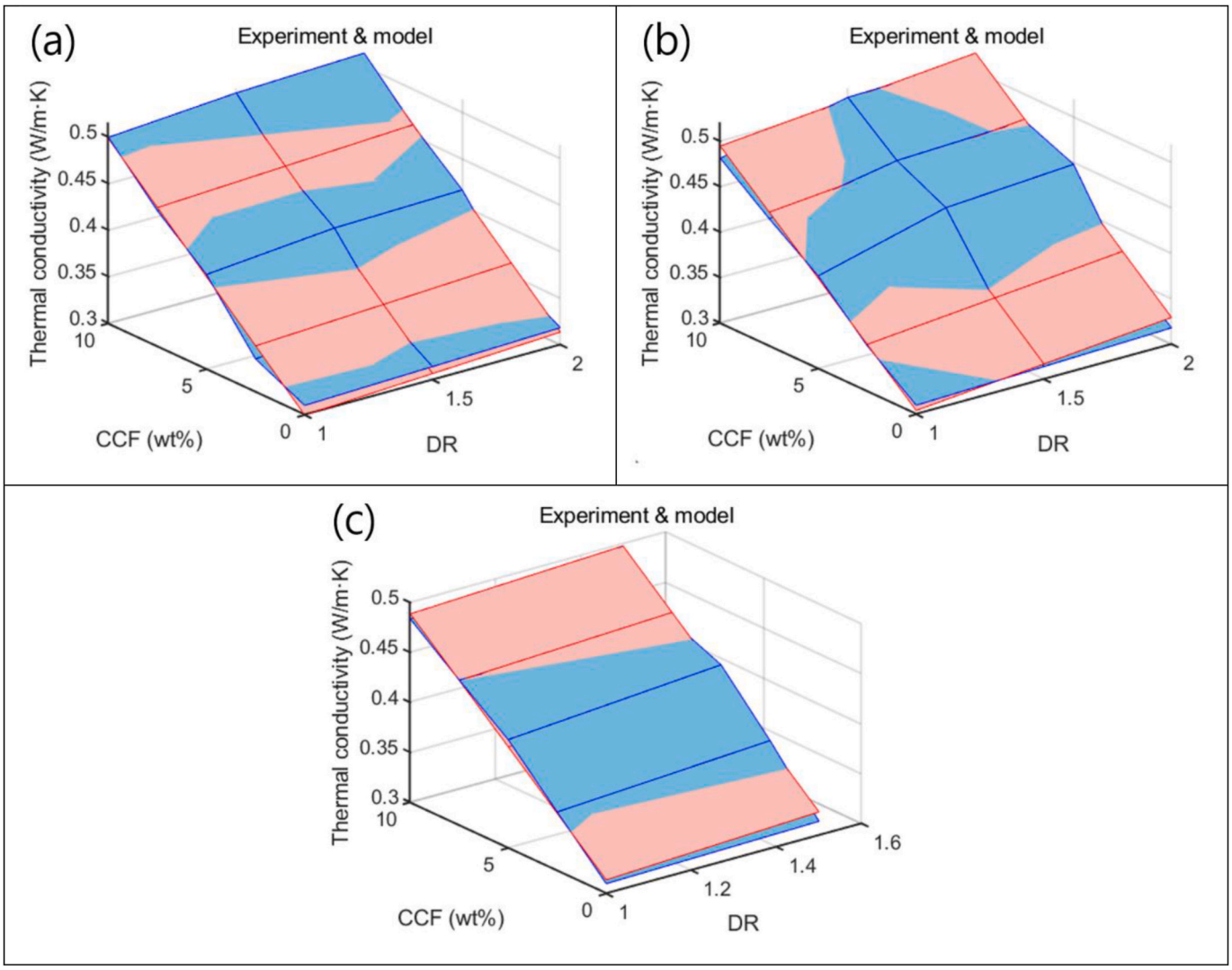

Fig. 7. Comparison of thermal conductivity values obtained through experiments and regression models: (a) 3 mm-CCF sample and Eq. (10), (b) 6 mm-CCF sample and Eq. (11), (c) 12 mm-CCF sample and Eq. (12).

Table 4
Average values of experimental results (unit: W/m·K).

wt.%	DR		
	1	1.5	2
0	0.31004	0.31396	0.31802
2.5	0.34486	0.353928	0.350333
5	0.3983625	0.419595	0.42432
7.5	0.4401925	0.452753	0.462473
10	0.48701	0.50298	0.509657

Overall, the thermal conductivity increased with the DR and CCF content. It can be observed that as the fibers are oriented according to the DR, the anisotropic properties of the composite material are enhanced, leading to increased thermal properties in the DR direction [15–17]. This change represents a composite property wherein the anisotropic properties are strengthened, despite the thermal conductivity of the carbon fiber remaining unchanged [18,19]. Figs. 4 and 5 show the variation in thermal conductivity with various parameters. The results indicate that the thermal conductivity increased with length. These observations align with those of Zang et al. who reported low vibrational losses during phonon movement within carbon fibers [20]. Notably, a significant enhancement in thermal conductivity was not observed owing to the increased energy required to induce phonon vibrations through coupling with high-molecular-weight HDPE. Thus, future endeavors may explore improvements in thermal conductivity through sizing and interfacial optimization of fibers [21].

The RSM, based on experimental data, was used to quantitatively analyze the thermal conductivity under different fiber contents, lengths, and DRs.

As shown in Fig. 4, as the CCF loading (wt.%) increased, the thermal conductivity increased. At a fixed DR of 1 and CCF concentrations of 2.5, 5, and 7.5 wt%, the thermal conductivity increased with the CCF length. For DR = 1.5, the CCF concentration increased with the fiber length when the CCF concentrations were 2.5 and 5 wt%. For DR = 2, the thermal conductivity increased with the length for all CCF contents. Thus, for large DR (e.g., DR = 2), the thermal conductivity may be expected to increase with the CCF length.

Fig. 5 shows that as the DR increased, the thermal conductivity increased at all CCF lengths. At a CCF concentration of 2.5 wt% (Fig. 5 (a)), the thermal conductivity increased with the CCF length. At 5 wt%, the thermal conductivity increased with the length. However, at DR 1.5, the thermal conductivity of the 12 mm-CCF sample was lower than that of the 6 mm-CCF sample (Fig. 5(b)). At 7.5 wt% (Fig. 5(c)), the thermal conductivity increased with the length at DR = 1 and 2. In the case of DR 1.5, the thermal conductivity of the 12 mm-CCF sample was lower than

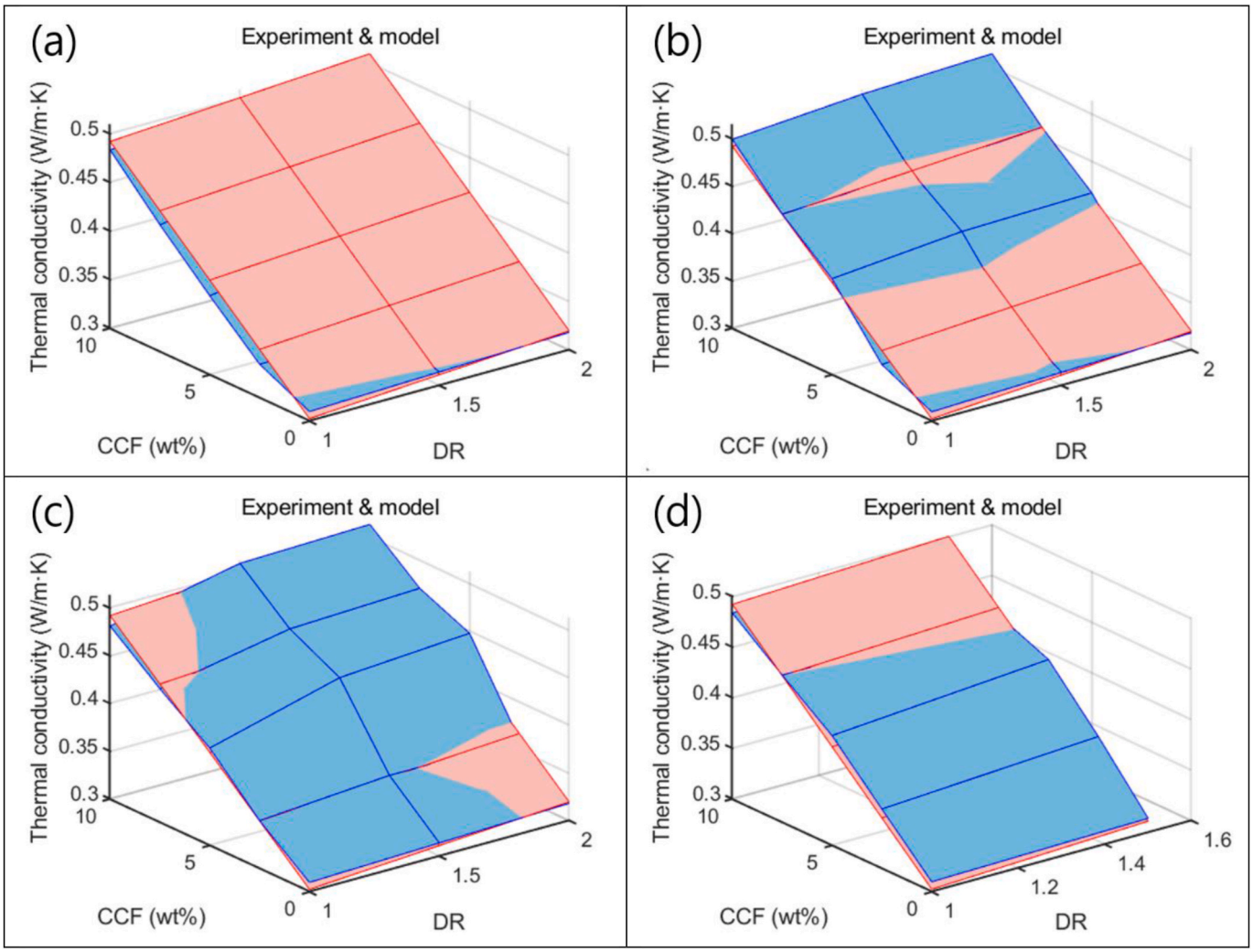

Fig. 8. Comparison of thermal conductivity values obtained through experiments and Eq. (13) model: (a) 1 mm-CCF sample, (b) 3 mm-CCF sample, (c) 6 mm-CCF sample, (d) 12 mm-CCF sample.

that of the 1, 3, and 6 mm-CCF samples. In other words, a consistent trend was not observed for DR 1.5. At a CCF content of 10 wt%, the thermal conductivity increased and then decreased as the length of CCF increased (Fig. 5(d)). This behavior may be attributable to a decrease in the degree of fiber alignment at larger CCF lengths and contents. This outcome is consistent with the findings of Huang et al. who observed similar trends in fiber orientation and distribution [22].

In summary, Figs. 4 and 5 show that with increase in the CCF content and DR, the thermal conductivity increased. At low CCF contents, the thermal conductivity increased as the CCF length increased across all DRs. However, at large CCF contents and large DR, the thermal conductivity increased with the CCF length.

3.2. RSM analysis with regression models

To examine the influence of the manufacturing parameters and establish a prediction model for the thermal conductivity of CCF/HDPE composites, linear regression models were determined using RSM. The vector **b** in Eq. (8) was obtained using the results provided in Table 2 and Eq. (7), as outlined in Table 3. Equations (10)–(13) define regressions models TC1, TC3, TC6, and TC12, used for predicting the thermal conductivity for composite samples with CCF lengths of 1, 3, 6, and 12 mm, respectively.

$$TC1 = 0.2786 + 0.0186 \times CCF(wt\%) + 0.0171 \times DR \quad (10)$$

$$TC3 = 0.2861 + 0.0199 \times CCF(wt\%) + 0.0136 \times DR \quad (11)$$

$$TC6 = 0.2791 + 0.0190 \times CCF(wt\%) + 0.0252 \times DR \quad (12)$$

$$TC12 = 0.2949 + 0.0175 \times CCF(wt\%) + 0.0190 \times DR \quad (13)$$

Fig. 6 presents a comparison of the experimental results of composites including 1 mm-CCF (Table 2) and model predictions Eq. (10) based on the CCF content and DR. The experimental and model results exhibited minimal errors and were reasonably consistent. In particular, the thermal conductivity increased with increasing CCF content and DR, as indicated by the positive coefficients of CCF content and DR in Eq. (10).

Fig. 7 presents a comparison of the experimental results of composites with CCF lengths of 3, 6, and 12 mm, and model predictions using Eqs (11)–(13). The small errors and close alignment between experimental and model results confirmed the accuracy of the predictive models.

In the case of Eqs. (10) and (11), the coefficient of CCF content was larger than that of DR, indicating that variance of composites with 1 mm- or 3 mm-CCF was more affected by the CCF content than the DR. In the case of composites with 6 mm- or 12 mm-CCF, Eqs. (12) and (13), the coefficient of the DR was greater than that of the CCF content, indicating the more notable influence of the DR on the deviation among the experimental results. In Eqs. (10)–(13), the standard deviations of the

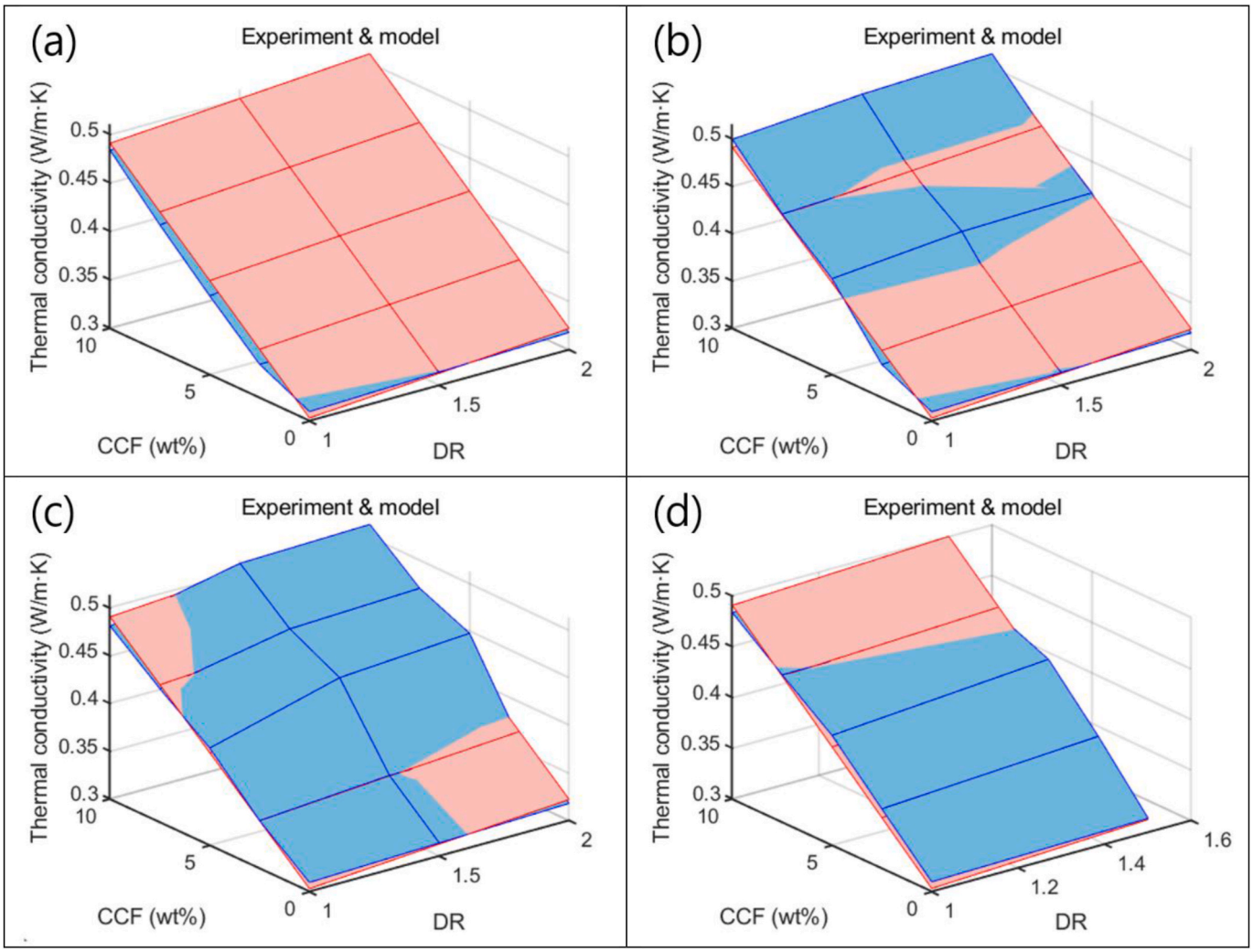

Fig. 9. Comparison of thermal conductivity values obtained through experiments and Eq. (14) model: (a) 1 mm-CCF sample, (b) 3 mm-CCF sample, (c) 6 mm-CCF sample, (d) 12 mm-CCF sample.

coefficients of CCF contents (0.0186, 0.0199, 0.0190, and 0.0175) and DR (0.0171, 0.0136, 0.0252, and 0.0190) were 9.95e-4 and 48.62e-4, respectively. These values indicated the more notable deviation associated with the DR, suggesting that DR exerted a greater influence than the CCF content on the discrepancy among the experimental results.

Table 4 presents the averages of the experimental results. The average value 0.34486 observed for CCF 2.5 wt% and DR 1 indicates the average of the experimental results for samples with CCF lengths of 1, 3, 6, and 12 mm (0.33475, 0.3353, 0.35042, and 0.35897, respectively) under identical conditions (Table 2). The other values were calculated in a similar manner. In the case of DR 2, as no result was available for the 12-mm CCF sample due to manufacturing difficulties, the average value was calculated using the experimental results of the 1, 3, and 6-mm CCF samples for the corresponding CCF wt%. The averages from Table 4 and Eq. (7) were used to identify the optimal regression model, as shown in Eq. (14). Fig. 8 shows a comparison between the results of this model and the experimental results presented in Table 2. The experimental results of the 1-mm sample were smaller than those of the model, whereas the results of the 3-mm sample were comparable with the model predictions. The results of the 6-mm sample were slightly larger than those obtained using the model. Therefore, overall, the thermal conductivity increased with the CCF length. However, according to the experimental results, under specific CCF contents and DRs, samples containing long CCFs exhibited lower thermal conductivity than those with shorter CCFs.

$$TC_{ave1} = 0.2858 + 0.0190 \times CCF(wt\%) + 0.0169 \times DR \quad (14)$$

Finally, we compared the experimental results with the regression model obtained using the average of each coefficient of different models. The mean values for the constant, coefficient of CCF content, and coefficient of DR, in Eqs. (10)–(13) were 0.2847, 0.0188, and 0.0187, respectively. Equation (15) shows the model constructed using these values.

$$TC_{ave2} = 0.2847 + 0.0188 \times CCF(wt\%) + 0.0187 \times DR \quad (15)$$

Fig. 9 presents a comparison of the results of this model with the experimental results presented in Table 2. The difference between the coefficients of Eqs. (15) and (14) was not significant, as indicated by the similarity of the results shown in Figs. 8 and 9.

Fig. 10 presents scanning electron microscopy (SEM) images illustrating the aligned morphology of CCF/HDPE composites. The length of the fiber was shortened by the shear force of the extruder [23,24], and the observed fiber looks shorter because the cross section was measured by cold fracture using liquid nitrogen [25]. At CCF contents of 5 and 10 wt%, varying numbers of carbon fibers were observed. At DR = 1, both compositions exhibited fibers arranged in a nearly random manner. However, at DR = 2, a highly aligned CCF structure was observed. This observation provides insights into the relationship between the CCF content and alignment, elucidating the rationale behind the observed

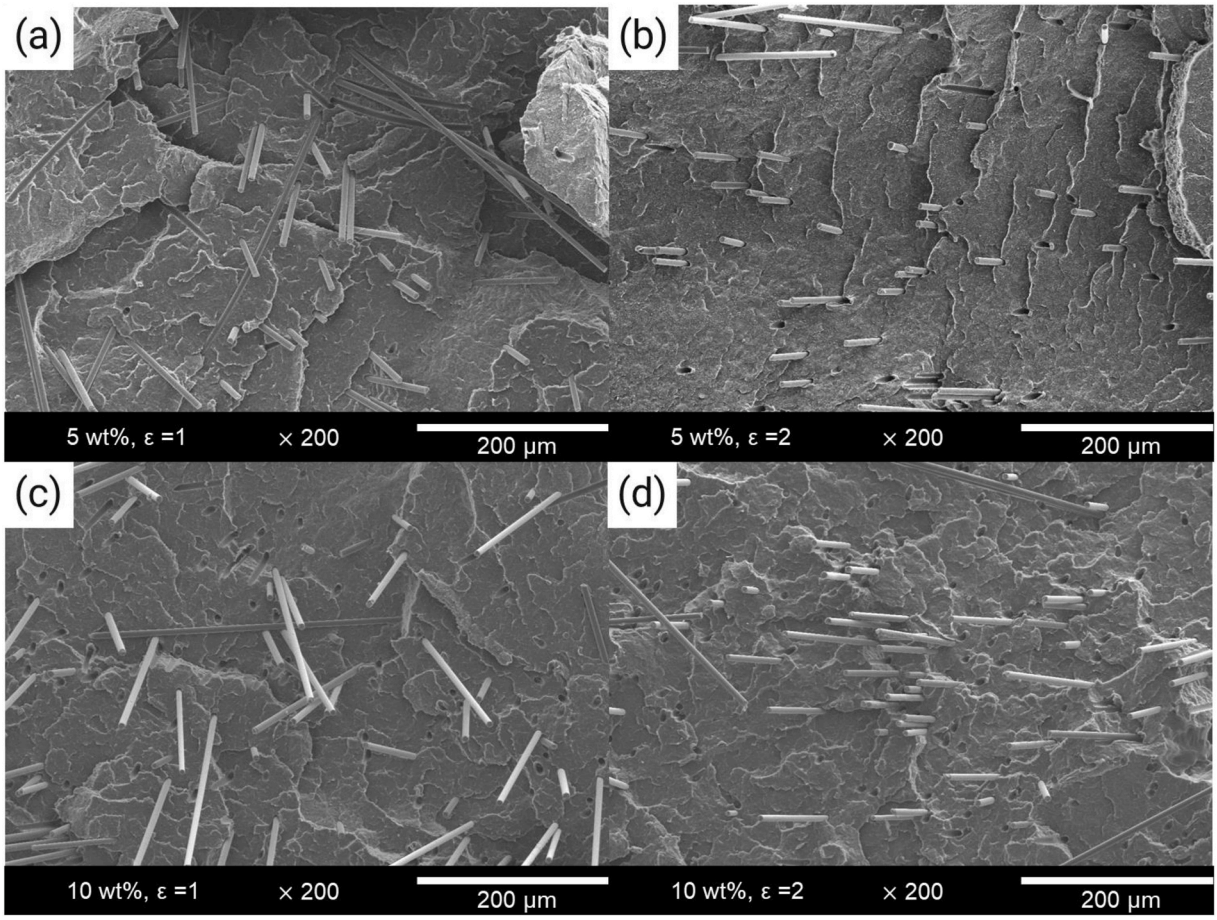

Fig. 10. SEM images depicting the morphological features of CCF/HDPE composites with (a), (b) fiber length of 6 mm, CCF concentration of 5 wt%, and different draw ratios; and (c), (d) fiber length of 6 mm, CCF concentration of 10 wt%, and different draw ratios.

increase in thermal conductivity.

4. Conclusions

This study was aimed at examining the thermal properties of unidirectionally aligned CCF/HDPE composites for applications requiring unidirectional heat dissipation. A special post-extrusion tension alignment method was used to fabricate the composite samples with aligned CCFs. The thermal conductivities were measured for various fiber contents, lengths, and DRs.

According to the experimental results, the thermal conductivity increased with increasing CCF content and DR. At low CCF contents (2.5 wt%), the thermal conductivity increased with the CCF length for all DRs. However, at large CCF contents (10 wt%), the thermal conductivity increased with increasing CCF length only at large DRs.

To assess the contribution of manufacturing variables, linear regression models were constructed using RSM. The model predictions were consistent with the experimental results. The variation in the thermal conductivity of 1 mm or 3 mm-CCF composites was more influenced by the CCF content than the DR. In contrast, the thermal conductivity of composites with 6 mm- or 12 mm-CCF was more influenced by the DR. Thus, the deviation among the experimental results was attributable more to DR than the CCF content. Moreover, according to the coefficient variances of the regression model, DR exerted a greater influence than the CCF content on the deviation among the experimental results.

The outcomes of the model obtained using the average results under each condition were similar to the experimental results for the 3 mm sample. However, the model yielded underestimated and overestimated values compared with the experimental results for the 1 mm and 6 mm samples, respectively. Overall, the thermal conductivity increased with the CCF length. However, according to the experimental results, depending on the CCF content and DR, samples with long CCFs exhibited lower thermal conductivity than samples with short CCFs.

The results of this study can provide a valuable foundation for the design and manufacturing of composite materials.

Funding

This research was supported by the Materials/Parts Technology Development Program (Grant No. 20017542) funded by the Ministry of Trade, Industry and Energy (MOTIE) of Korea through the Korea Evaluation Institute of Industrial Technology (KEIT), by the National Research Foundation of Korea (NRF) funded by the Ministry of Science and ICT (MSIT) of Korea (No. 2021R1F1A1051836), and by the National Research Council of Science and Technology (NST) grant funded by MSIT (No. CRC23011-000).

CRediT authorship contribution statement

Gu-Hyeok Kang: Writing – original draft, Methodology, Formal analysis, Data curation, Conceptualization. **Myungsoo Kim:** Writing – review & editing, Writing – original draft, Visualization, Supervision, Funding acquisition, Formal analysis, Data curation. **Young-Bin Park:** Writing – review & editing, Supervision, Resources, Project administration, Investigation, Funding acquisition.

Declaration of competing interest

The authors declare that they have no known competing financial interests or personal relationships that could have appeared to influence the work reported in this paper.

Data availability

Data will be made available on request.

References

[1] Y. Lv, G. Zhang, Q. Wang, W. Chu, Thermal management technologies used for high heat flux automobiles and aircraft: a review, Energies 15 (21) (2022) 8316.
[2] D. Faulkner, M. Khotan, R. Shekarriz, Managing electronics thermal management, Heat Tran. Eng. 25 (2) (2004) 1–4.
[3] O. Erixno, N. Abd Rahim, F. Ramadhani, N.N. Adzman, Energy management of renewable energy-based combined heat and power systems: a review, Sustain. Energy Technol. Assessments 51 (2022) 101944.
[4] S.N. David Chua, B.K. Chan, S.F. Lim, Experimental and simulation study of thermal accumulation in an enclosed vehicle, Proc. Inst. Mech. Eng. D: J. Automob. Eng. 233 (14) (2019) 3621–3629.
[5] A.A. Almubarak, The effects of heat on electronic components, Int. J. Eng. Res. Afr. 7 (5) (2017) 52–57.
[6] M. Vadivelu, C.R. Kumar, G.M. Joshi, Polymer composites for thermal management: a review, Compos. Interfac. 23 (9) (2016) 847–872.
[7] Y. Agari, A. Ueda, S. Nagai, Thermal conductivities of composites in several types of dispersion systems, J. Appl. Polym. Sci. 42 (6) (1991) 1665–1669.
[8] N. Burger, A. Laachachi, M. Ferriol, M. Lutz, V. Toniazzo, D. Ruch, Review of thermal conductivity in composites: mechanisms, parameters and theory, Prog. Polym. Sci. 61 (2016) 1–28.
[9] M. Zhou, S. Tan, J. Wang, Y. Wu, L. Liang, G. Ji, "Three-in-one" multi-scale structural design of carbon fiber-based composites for personal electromagnetic protection and thermal management, Nano-Micro Lett. 15 (1) (2023) 176.
[10] Y. Ibrahim, A. Elkholy, J.S. Schofield, G.W. Melenka, R. Kempers, Effective thermal conductivity of 3D-printed continuous fiber polymer composites, Adv. Manuf. Polym. Compos. Sci. 6 (1) (2020) 17–28.
[11] Q. Gao, M. Jing, M. Chen, S. Zhao, W. Wang, J. Qin, C. Wang, Microfibril alignment induced by stretching fields during the dry-jet wet spinning process: reinforcement on polyacrylonitrile fiber mechanical properties, Polym. Test. 81 (2020) 106191.
[12] O. Adole, L. Anguilano, T. Minton, J. Campbell, L. Sean, S. Valisios, K. Tarverdi, Basalt fibre-reinforced high density polyethylene composite development using the twin screw extrusion process, Polym. Test. 91 (2020) 106467.
[13] M.A.G. Benega, W.M. Silva, M.C. Schnitzler, R.J.E. Andrade, H. Ribeiro, Improvements in thermal and mechanical properties of composites based on epoxy-carbon nanomaterials-A brief landscape, Polym. Test. 98 (2021) 107180.
[14] R.H. Myers, D.C. Montgomery, C.M. Anderson-Cook, Response Surface Methodology: Process and Product Optimization Using Designed Experiments, John Wiley & Sons, 2016.
[15] G.-H. Kang, C. Joung, M. Kim, Y.-B. Park, Novel method of mechanical alignment for chopped carbon fiber/high density polyethylene composites: processing, modeling, and characterization, Composites Part C: Open Access 12 (2023) 100400.
[16] M. Qu, F. Nilsson, D.W. Schubert, Effect of filler orientation on the electrical conductivity of carbon Fiber/PMMA composites, Fibers 6 (2018) 3.
[17] S.-B. Min, M. Kim, K. Hyun, C.-W. Ahn, C.B. Kim, Thermally conductive 2D filler orientation control in polymer using thermophoresis, Polym. Test. 117 (2023) 107838.
[18] W. Lee, J. Kim, Improved thermal conductivity of poly (dimethylsiloxane) composites filled with well-aligned hybrid filler network of boron nitride and graphene oxide, Polym. Test. 104 (2021) 107402.
[19] V. Gavande, S. Nagappan, B. Seo, Y.-S. Cho, W.-K. Lee, Transparent nylon 6 nanofibers-reinforced epoxy matrix composites with superior mechanical and thermal properties, Polym. Test. 122 (2023) 108002.
[20] X. Zhang, S. Fujiwara, M. Fujii, Measurements of thermal conductivity and electrical conductivity of a single carbon fiber, Int. J. Thermophys. 21 (2000) 965–980.
[21] C. Cheng, M. Zhang, S. Wang, Y. Li, H. Feng, D. Bu, Z. Xu, Y. Liu, L. Jin, L. Xiao, Y. Ao, Improving interfacial properties and thermal conductivity of carbon fiber/epoxy composites via the solvent-free GO@ Fe3O4 nanofluid modified water-based sizing agent, Compos. Sci. Technol. 209 (2021) 108788.
[22] H. Huang, X. Gao, K.H. Khayat, A. Su, Influence of fiber alignment and length on flexural properties of UHPC, Construct. Build. Mater. 290 (2021) 122863.
[23] A. Rüppel, S. Wolff, J.P. Oldemeier, V. Schöppner, H.-P. Heim, Influence of processing glass-fiber filled plastics on different twin-screw extruders and varying screw designs on fiber length and particle distribution, Polymers 14 (2022) 3113.
[24] F. Inceoglu, J. Ville, N. Ghamri, A. Durin, R. Valette, B. Vergnes, A study of fiber breakage during compounding of glass fiber reinforced composites, in: Proceedings of the Polymer Processing Society 26th Annual Meeting, Banff, AB, Canada, 2010, pp. 4–8.
[25] A. Kaushal, V. Singh, Analysis of mechanical, thermal, electrical and EMI shielding properties of graphite/carbon fiber reinforced polypropylene composites prepared via a twin screw extruder, J. Appl. Polym. Sci. 139 (2022) 51444.